

Hadronic Production of Λ_c from 600 GeV/c π^- , Σ^- and p beams

F.G. Garcia^{19,5}, G. Alkhazov¹¹, A.G. Atamantchouk^{11,*}, M.Y. Balatz^{8,*}, N.F. Bondar¹¹, P.S. Cooper⁵, L.J. Dauwe¹⁷, G.V. Davidenko⁸, U. Dersch^{9,†}, A.G. Dolgolenko⁸, G.B. Dzyubenko⁸, R. Edelman³, L. Emediato¹⁹, A.M.F. Endler⁴, J. Engelfried^{13,5}, I. Eschrich^{9,‡}, C.O. Escobar^{19,§}, A.V. Evdokimov⁸, I.S. Filimonov^{10,*}, M. Gaspero¹⁸, I. Giller¹², V.L. Golovtsov¹¹, P. Gouffon¹⁹, E. Gülmez², He Kangling⁷, M. Iori¹⁸, S.Y. Jun³, M. Kaya¹⁶, J. Kilmer⁵, V.T. Kim¹¹, L.M. Kochenda¹¹, I. Konorov^{9,¶}, A.P. Kozhevnikov⁶, A.G. Krivshich¹¹, H. Krüger^{9,||}, M.A. Kubantsev⁸, V.P. Kubarovsky⁶, A.I. Kulyavtsev^{3,5}, N.P. Kuropatkin^{11,5}, V.F. Kurshetsov⁶, A. Kushnirenko³, S. Kwan⁵, J. Lach⁵, A. Lamberto²⁰, L.G. Landsberg⁶, I. Larin⁸, E.M. Leikin¹⁰, Li Yunshan⁷, M. Luksys¹⁴, T. Lungov^{19,**}, V.P. Maleev¹¹, D. Mao^{3,††}, Mao Chensheng⁷, Mao Zhenlin⁷, P. Mathew^{3,‡‡}, M. Mattson³, V. Matveev⁸, E. McCliment¹⁶, M.A. Moinester¹², V.V. Molchanov⁶, A. Morelos¹³, K.D. Nelson^{16,§§}, A.V. Nemitkin¹⁰, P.V. Neoustroev¹¹, C. Newsom¹⁶, A.P. Nilov⁸, S.B. Nurushev⁶, A. Ocherashvili¹², Y. Onel¹⁶, E. Ozel¹⁶, S. Ozkorucuklu¹⁶, A. Penzo²⁰, S.V. Petrenko⁶, P. Pogodin¹⁶, M. Procario^{3,¶¶}, V.A. Prutskoi⁸, E. Ramberg⁵, G.F. Rappazzo²⁰, B.V. Razmyslovich¹¹, V.I. Rud¹⁰, J. Russ³, P. Schiavon²⁰, J. Simon^{9,***}, A.I. Sitnikov⁸, D. Skow⁵, V.J. Smith¹⁵, M. Srivastava¹⁹, V. Steiner¹², V. Stepanov¹¹, L. Stutte⁵, M. Svoiski¹¹, N.K. Terentyev^{11,3}, G.P. Thomas¹, L.N. Uvarov¹¹, A.N. Vasiliev⁶, D.V. Vavilov⁶, V.S. Verebryusov⁸, V.A. Victorov⁶, V.E. Vishnyakov⁸, A.A. Vorobyov¹¹, K. Vorwalter^{9,†††}, J. You^{3,5}, Zhao Wenheng⁷, Zheng Shuchen⁷, R. Zukanovich-Funchal¹⁹

(SELEX Collaboration)

¹Ball State University, Muncie, IN 47306, U.S.A.²Bogazici University, Bebek 80815 Istanbul, Turkey³Carnegie-Mellon University, Pittsburgh, PA 15213, U.S.A.⁴Centro Brasileiro de Pesquisas Físicas, Rio de Janeiro, Brazil⁵Fermilab, Batavia, IL 60510, U.S.A.⁶Institute for High Energy Physics, Protvino, Russia⁷Institute of High Energy Physics, Beijing, P.R. China⁸Institute of Theoretical and Experimental Physics, Moscow, Russia⁹Max-Planck-Institut für Kernphysik, 69117 Heidelberg, Germany¹⁰Moscow State University, Moscow, Russia¹¹Petersburg Nuclear Physics Institute, St. Petersburg, Russia¹²Tel Aviv University, 69978 Ramat Aviv, Israel¹³Universidad Autónoma de San Luis Potosí, San Luis Potosí, Mexico¹⁴Universidade Federal da Paraíba, Paraíba, Brazil¹⁵University of Bristol, Bristol BS8 1TL, United Kingdom¹⁶University of Iowa, Iowa City, IA 52242, U.S.A.¹⁷University of Michigan-Flint, Flint, MI 48502, U.S.A.¹⁸University of Rome "La Sapienza" and INFN, Rome, Italy¹⁹University of São Paulo, São Paulo, Brazil²⁰University of Trieste and INFN, Trieste, Italy

(November 17, 2018)

We present data from Fermilab experiment E781 (SELEX) on the hadroproduction asymmetry for $\bar{\Lambda}_c^-$ compared to Λ_c^+ as a function of x_F and p_t^2 distributions for Λ_c^+ . These data were measured in the same apparatus using incident π^- , Σ^- beams at 600 GeV/c and proton beam at 540 GeV/c. The asymmetry is studied as a function of x_F . In the forward hemisphere with $x_F \geq 0.2$ both baryon beams exhibit very strong preference for producing charm baryons rather than charm antibaryons, while the pion beam asymmetry is much smaller. In this energy regime the results show that beam fragments play a major role in the kinematics of Λ_c formation, as suggested by the leading quark picture.

I. INTRODUCTION

The conventional leading order (LO) and next to leading order (NLO) charm-anticharm production diagrams at the quark level show little or no asymmetry in the x_F or p_t behaviour of the quark and antiquark, as viewed in the laboratory frame. Previous studies, primarily using pion beams at a variety of energies up to 500 GeV/ c , have shown that in many cases charm mesons that share a quark in common with the beam hadron, so-called *leading charm*, are produced more copiously in the forward hemisphere than those states which do not have a shared quark, i.e., *non-leading charm* [1]. Recently, this has been extended to charm baryon production by a Σ^- beam, where asymmetry for Λ_c^+ compared to $\bar{\Lambda}_c^-$ as a function of x_F was reported to be large [2]. There are limited-statistics proton data available for central production, where only a 90% confidence level lower limit is reported [3].

Because the quark-level processes are thought to be symmetric, the asymmetries are viewed as features of the hadronization process [4] or as a manifestation of an intrinsic charm content of the beam hadron [5]. In this experiment the Λ_c^+ shares a quark in common with all three beam hadrons, while the antibaryon has an antiquark in common with the π^- beam only. We shall compare the hadroproduction characteristics for these charm baryon and antibaryon states to illuminate the role of the beam fragments in hadronization induced asymmetries.

II. APPARATUS DESCRIPTION

The SELEX spectrometer is a three-stage magnetic spectrometer designed to cover charm production in the forward hemisphere. The beam hadron was identified by a transition radiation detector as pion or not-pion and tracked in 8 beam silicon strip detectors before interacting in a set of 5 target foils, 2 copper and 3 carbon totalling 5% of a proton interaction length. Interaction products were tracked in a set of 20 vertex silicon detectors arranged in 4 sets of planes rotated by 45°. Single-track efficiencies for each system exceeded 98%. Data were taken with negative beam at 615 GeV/ c (half π , half Σ) totalling 12.3×10^9 inelastic interactions and positive beam at 540 GeV/ c (92% protons) totalling 2.8×10^9 inelastic interactions. The layout of the spectrometer can be found elsewhere [6].

Two Proportional Wire Chamber (PWC) magnetic spectrometer systems analyzed tracks with momenta above 3 GeV/ c (M1 spectrometer, 12 planes) or 15 GeV/ c (M2 spectrometer, 14 planes). The beam region of the PWCs was covered with double-sided silicon detectors to give high-resolution momentum measurement up to full

beam energy. The combination of excellent vertex-region tracking resolution (typically 65 μrad at 150 GeV/ c) and excellent momentum resolution ($\sigma_p/p \approx 0.5\%$ for a typical 100 GeV/ c track) gave a Λ_c^+ mass resolution (σ) of about 9 MeV/ c^2 at all x_F . Tracks above 22 GeV/ c traversed a Ring-Imaging Čerenkov (RICH) and were identified as π , K, or p [7]. The RICH distinguished K^\pm from π^\pm up to 165 GeV/ c . The proton identification efficiency was greater than 95 % above proton threshold (≈ 90 GeV/ c) and greater than 90 % above kaon threshold (≈ 45 GeV/ c).

An important innovation in SELEX was the use of an online topological trigger to identify charm. The hardware trigger was loose, requiring ≥ 4 charged hadrons in the forward 150 mrad cone and ≥ 2 hits from positive track candidates in a hodoscope after M2. About 1/3 of all inelastic interactions satisfied this trigger. The software trigger made a full vertex reconstruction of the beam track and all tracks in the M2 spectrometer (high momentum tracks) to test that hypothesis that they all came from a single primary vertex. A software-adjustable χ^2 cut of 8.5 selected candidate events that were inconsistent with a single primary vertex, i.e., events that *might* have a downstream decay. This gave a rejection factor of about 8 in the data volume. Studies with the software trigger turned off show that this costs about a factor of 2 in charm efficiency, for a net filter enhancement of 4.

III. DATA ANALYSIS

A general data reduction pass found reconstructable charged tracks and identified the interacting beam track. Primary and secondary vertices were found by geometric reconstruction without regard to particle identification. The high resolution of the beam and vertex systems, along with the thin production targets, gave typical primary vertex resolution of 270 μm and secondary vertex resolution for these Λ_c^+ events of 560 μm for a mean Λ_c^+ momentum of 230 GeV/ c .

All the $pK\pi$ candidates used in this analysis were selected by the following requirements: (1) primary and secondary vertex fits each had $\chi^2/\text{dof} < 5$; (2) the primary-secondary vertex separation significance (L/σ) had to be greater than 8, where σ is the quadrature sum of the primary and secondary vertex errors; (3) the total momentum vector of the decay tracks had to point back to the primary vertex within errors; (4) ($\bar{\Lambda}_c^-$) Λ_c^+ events were required to have positive RICH identification for the (anti)proton and the $(K^+)K^-$. The pion could be any track; (5) secondary vertices which occurred inside any target were removed; (6) each secondary track was extrapolated back to the primary vertex to determine its transverse miss distance. The second-largest transverse miss distance had to exceed 20 μm .

Events were selected by the above cuts and sorted by the primary beam tag: Σ^- or π^- from the negative beam and protons from the positive beam. Figure 1 shows the full SELEX statistics for the $\bar{\Lambda}_c^- \rightarrow \bar{p}K^+\pi^-$ and $\Lambda_c^+ \rightarrow pK^-\pi^+$ mass plots where signals for all beams are combined. Gaussian fits are shown for illustration

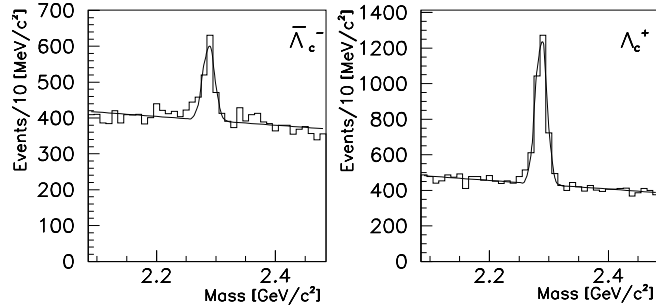


FIG. 1. Mass distributions for $\bar{\Lambda}_c^-$ (left) and Λ_c^+ (right) where signals for all beams are combined. Gaussian fits are shown for illustration only.

only. The background shapes are smooth on the low mass and high mass side of the signal regions. The signal yield for baryons and antibaryons are determined by a side-band subtraction method which assumes a linear mass resolution dependence for the momentum spectrum. The number of background events estimated outside the signal window is subtracted from the number of events in the signal window. The signal window corresponds to a $3.33\text{-}\sigma$ mass width and the background is $10\text{-}\sigma$ centered at $2.285\text{ GeV}/c^2$. We find 1979 ± 71 signal events for Λ_c^+ and 520 ± 60 signal events for $\bar{\Lambda}_c^-$.

IV. ASYMMETRY ANALYSIS AND x_F DISTRIBUTIONS

The data yields were corrected in each x_F bin by the total acceptance (geometrical acceptance and reconstruction efficiency). The simulation used Monte Carlo generated Λ_c^+ (or c.c.) events with phase space decay to the $pK\pi$ final state. The simulated trajectories were converted to hits in all tracking detectors, including multiple Coulomb scattering but not secondary interaction losses. The hits were embedded in the hit banks of real data and all tracks were reconstructed. This overestimates slightly the tracking inefficiency, but this effect is small. The RICH simulation has been tested against a set of $\Lambda^0 \rightarrow p + \pi^-$ events taken without a RICH cut. Agreement is excellent; the proton identification efficiency averaged over the momentum spectrum is 95%.

The simulated events were analysed with the same tracking and reconstruction procedure used in the data. The whole set of cuts used to extract the signal was applied here as well. The acceptance is the ratio between

Beam particle	Λ_c^+		$\bar{\Lambda}_c^-$	
	x_F	n - value	x_F	n - value
π^-	0.15 - 0.85	2.65 ± 0.44	0.15 - 0.675	2.2 ± 0.8
Σ^-	0.125 - 0.925	2.45 ± 0.18	0.125 - 0.825	6.8 ± 1.1
p	0.15 - 0.85	2.33 ± 0.30	0.15 - 0.60	no fit

TABLE I. Summary of measured n-value from the fit $(1 - x_F)^n$ for Λ_c^+ and $\bar{\Lambda}_c^-$. The errors are statistical only.

the number of events reconstructed by the number of embedded events generated. SELEX acceptance does not depend on the transverse momentum of the charm particle up to $p_t^2 = 7\text{ (GeV}/c)^2$. Therefore we consider only the acceptance as a function of x_F . An important issue for this analysis is the relative efficiency for the baryon and antibaryon decays. As seen in figure 2, there is no discernable difference in the acceptances. The x_F distribution of the acceptance-corrected number of events from each beam is shown in figure 3. Because the beam flux is the same for baryon and antibaryon, these figures compare the relative production cross sections for these states. The curves shown are fits of the standard parametrization $(1 - x_F)^n$ to the data. The results are summarized in table I. The relative sizes of the differen-

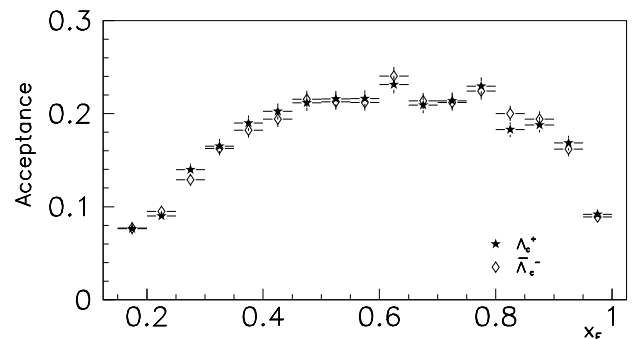


FIG. 2. Acceptance of Λ_c reconstruction.

tial cross sections for baryon and anti-baryon production are clearly different for pion and baryon beams. The pion beam valence quark content is baryon/antibaryon symmetric. Relative cross sections for Λ_c^+ and $\bar{\Lambda}_c^-$ production from pions are comparable in shape and magnitude over the entire x_F range. Such behaviour is consistent with the leading particle picture, since both charm states share a valence quark in common with the beam. For Σ^- and proton beams Λ_c^+ production is much stronger than $\bar{\Lambda}_c^-$ production, especially at high x_F . In this case there are no valence antiquarks, and antibaryon production appears to be strongly disfavored. The four distributions that show leading behaviour are consistent with a common $(1 - x_F)^n$ dependence having $n \sim 2.5$, much harder than the n for leading meson production from pion beams [8,9]. Note that the high-statistics Σ^- distribution shows some interesting structures. Clearly Λ_c^+

production is favored over $\bar{\Lambda}_c^-$, and the enhancement increases with x_F . The p_t^2 spectrum for Λ_c^+ production by

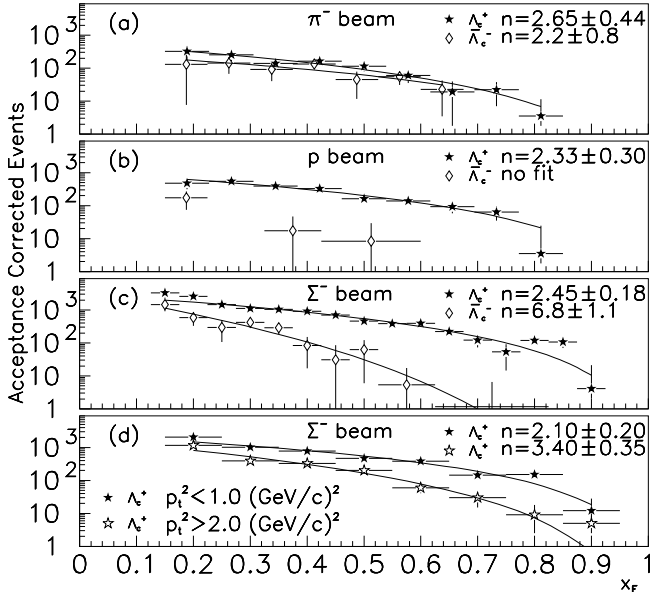


FIG. 3. Λ_c x_F distribution of corrected number of events for π^- (a), proton (b) and Σ^- (c) beams. (d) shows the Λ_c^+ x_F distribution for Σ^- production at low p_t^2 and high p_t^2 .

the three different beam hadrons is shown in Fig. 4. For $p_t^2 \leq 2$ (GeV/c) 2 all three beams are consistent with a smooth exponential spectrum $e^{-bp_t^2}$ with the same parameter $b \approx 1.1$ (GeV/c) $^{-2}$. At larger p_t^2 values, seen only in the high-statistics Σ^- data, the exponential gives way to a power-law behavior as expected in QCD and as seen in $D^{\pm,0}$ production [8]. There is no indication in the large- x_F events of an enhancement at small p_t^2 as suggested by the intrinsic charm picture. However, when we look at the x_F behaviour of events after the slope change at $p_t^2 \geq 2$ (GeV/c) 2 , we see a significant difference in the x_F behaviour. The events with large p_t^2 have a softer x_F spectrum than those at small p_t^2 , as seen in figure 3 (d). The hadroproduction asymmetry A is defined as:

$$A \equiv \frac{\sigma_c - \sigma_{\bar{c}}}{\sigma_c + \sigma_{\bar{c}}} \quad (1)$$

where σ_c ($\sigma_{\bar{c}}$) is the production cross-section for the charm particle (anti-charm particle) in study.

We calculated the values of the asymmetry and the errors using the maximum likelihood method with no limit at $A = \pm 1$. Events in each x_F bin follow the Poisson distribution. Therefore, the likelihood function is a product between two Poisson distributions, one for the background region and the other for the signal region.

The results are presented for the three beam hadrons in figure 5. As is already clear from the x_F distributions, Λ_c production in Σ^- and proton beams shows a strong asymmetry favoring baryons over antibaryons at all x_F .

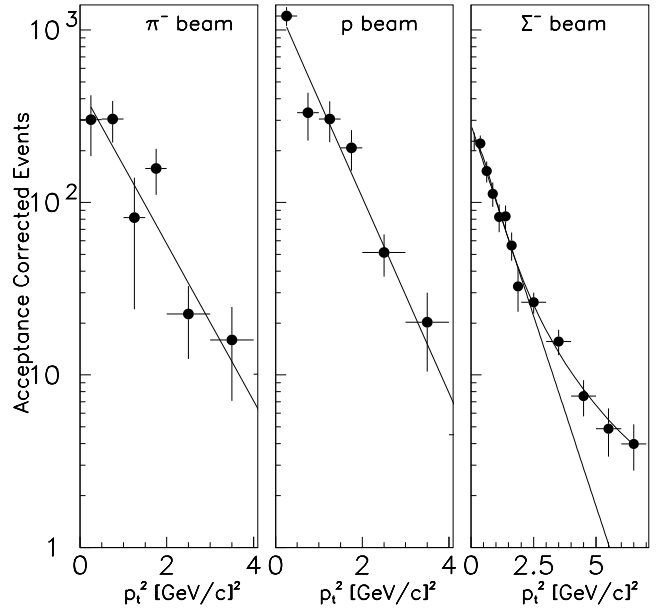


FIG. 4. Λ_c p_t^2 distribution of corrected number of events for π^- (left), proton (center) and Σ^- (right) beams.

The proton asymmetry rises sharply toward unity already at small x_F , reflective of the paucity of $\bar{\Lambda}_c^-$ production by protons. The Σ^- asymmetry has a smoother approach to the limit at +1. In the case of the π^- beam we see only a slightly positive and constant asymmetry throughout the x_F range. Our result agrees well in the overlap region with recent E791 data [10].

V. SYSTEMATIC ERRORS

Systematic errors in kinematic analysis may arise from several sources. We list here the ones that have been considered. In all cases systematic effects are found to be small compared to statistical errors.

- x_F binning effects

The x_F distribution is relatively smooth, but there are structures in the high statistics data. We have shifted the bin limits for all x_F distributions by 0.025 (half a bin) and refit the data. No effect in the character of the distributions is observed. For example, all the structures seen in Fig.3(c) are also present in the shifted distribution. Changes in the n -value are consistent with purely-statistical effects. Therefore, we quote a conservative Δn for the fit of 0.1, even though no systematic effect has been seen.

- Mass window size

The signal window in the mass distribution is taken as ± 30 MeV/ c^2 around 2.285 GeV/ c^2 . We have

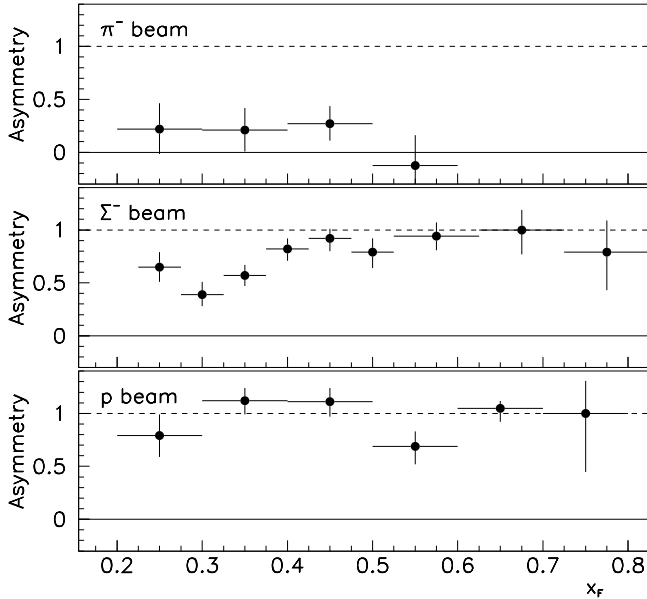


FIG. 5. Asymmetry for Λ_c production by π^- (top), Σ^- (center) and proton (bottom) beam.

changed the window up to $\pm 35 \text{ MeV}/c^2$ and down to $\pm 25 \text{ MeV}/c^2$. The systematic error for changing the mass window compared to statistical error is negligible.

- Acceptance correction

The acceptance shown in Fig. 2 is computed using the method of adding hits from simulated charm decay tracks into the data banks from an observed event. The modified event is reanalysed to see if the charm state is reconstructed. There could be a shift in the corrected x_F distribution if the acceptance calculation does not represent truly the x_F variation of the apparatus efficiency. In E781 the dominant efficiency variation at low x_F is purely geometric: both proton and kaon pass through the fiducial volume of the RICH counter. A second geometric effect is the related one: the charm particle live long enough to pass the vertex significance cut. The tracking characteristics of the spectrometer match those predicted from the simulation very well over all momenta studied here. The K_s mass is the same for all observed momenta, both in data and simulation. We believe that there is no systematic bias from the simulation and assign no error.

- Trigger Bias in Asymmetry

The x_F -dependent effects tend to cancel in the asymmetry measurement. However, a new systematic effect must be considered: Trigger bias. The E781 trigger required counts on the positive-bend side of a trigger hodoscope after the second bending magnet. This *might* favor Λ_c^+ production over

Λ_c^+ . We looked at the asymmetry of K_s production, for times when the π^+ is found in the high-momentum spectrometer compare to the converse. We see a maximum 3% asymmetry. We also look at the charm baryon data itself. If we exclude the charm tracks, then in 97% of the triggers there are still enough hits in the hodoscope to trigger the event without the charm decay tracks. We conservatively assign a 3% systematic error to the asymmetry from trigger bias.

VI. SUMMARY

The SELEX experiment reconstructed about 2500 $\Lambda_c \rightarrow pK\pi$ from 600 GeV/c Σ^- and π^- beams and a 540 GeV/c proton beam. We observed that the x_F -dependence of Λ_c^+ production is similar for all three beams, much stiffer than for meson production. Both baryon beams show a strong enhancement of the production of charm baryons over antibaryons, while the two are produced comparably from a pion beam. These results are in general agreement with color-drag models of hadronization. The differences in behaviour for protons and Σ^- illustrate significant non-perturbative effects in production dynamics at these energies.

The authors are indebted to the staff of Fermi National Accelerator Laboratory and for invaluable technical support from the staffs of collaborating institutions. This project was supported in part by Bundesministerium für Bildung, Wissenschaft, Forschung und Technologie, Consejo Nacional de Ciencia y Tecnología (CONACyT), Conselho Nacional de Desenvolvimento Científico e Tecnológico, Fondo de Apoyo a la Investigación (UASLP), Fundação de Amparo à Pesquisa do Estado de São Paulo (FAPESP), the Israel Science Foundation founded by the Israel Academy of Sciences and Humanities, Istituto Nazionale di Fisica Nucleare (INFN), the International Science Foundation (ISF), the National Science Foundation (Phy #9602178), NATO (grant CR6.941058-1360/94), the Russian Academy of Science, the Russian Ministry of Science and Technology, the Turkish Scientific and Technological Research Board (TÜBİTAK), the U.S. Department of Energy (DOE grant DE-FG02-91ER40664 and DOE contract number DE-AC02-76CHO3000), and the U.S.-Israel Binational Science Foundation (BSF).

* deceased

† Present address: Infineon, München, Germany

‡ Now at Imperial College, London SW7 2BZ, U.K.

- § Now at Instituto de Física da Universidade Estadual de Campinas, UNICAMP, SP, Brazil
- ¶ Now at Physik-Department, Technische Universität München, 85748 Garching, Germany
- || Present address: The Boston Consulting Group, München, Germany
- ** Now at Instituto de Física Teórica da Universidade Estadual Paulista, São Paulo, Brazil
- †† Present address: Lucent Technologies, Naperville, IL
- ‡‡ Present address: SPSS Inc., Chicago, IL
- §§ Now at University of Alabama at Birmingham, Birmingham, AL 35294
- ¶¶ Present address: DOE, Germantown, MD
- *** Present address: Siemens Medizintechnik, Erlangen, Germany
- ††† Present address: Deutsche Bank AG, Eschborn, Germany

- [1] E.M. Aitala *et al.*, Phys. Lett. **B371**, 157 (1996).
- [2] M.I. Adamovich *et al.*, Eur. Phys. J. **C8**, 593 (1999).
- [3] G.A. Alves *et al.*, Phys. Lett. **77**, 2388 (1996).
- [4] E. Norrbin and T. Sjostrand, Phys. Lett. **B442**, 407 (1998).
- [5] R. Vogt and S.J. Brodsky, Nucl. Phys. **B438**, 261 (1995).
- [6] SELEX Collaboration, J.S. Russ *et al.*, in *Proceedings of the 29th International Conference on High Energy Physics*, 1998, edited by A. Astbury *et al.* (World Scientific, Singapore, 1998), Vol. II, p. 1259; hep-ex/9812031.
- [7] J. Engelfried *et al.*, Nucl. Instrum. Methods A **431**, 53 (1999).
- [8] BEATRICE Collaboration, M. Adamovich, *et al.*, Nucl. Phys. B495 (1997)3; E791 Collaboration, E. M. Aitala, *et al.*, Phys. Lett. B462 (1999)225
- [9] E769 Collaboration, G.A. Alves, *et al.*, Phys. Rev. Lett. **77** (1996) 2392.
- [10] E791 Collaboration, *et al.*, in *Proceedings of Heavy Quark at Fixed Target*, 1998, edited by H.W.K. Cheung *et al.* (AIP Conference Proceedings, Springer-Verlag, 1999), Vol. 459, p. 159.